Journal of Sports Sciences, January 2006; 24(1): 11 – 22

Taylor & Francis
Taylor & Francis Group

Impact phase kinematics of instep kicking in soccer

HIROYUKI NUNOME[1], MARK LAKE[2], APOSTOLOS GEORGAKIS[3], & LAMPROS K. STERGIOULAS[4]

[1]*Research Centre of Health, Physical Fitness and Sports, Nagoya University, Nagoya, Japan,* [2]*Research Institute for Sport and Exercise Sciences, Liverpool John Moores University, Liverpool, UK,* [3]*Division of Engineering, King's College, London, UK and* [4]*Department of Information Systems and Computing, Brunel University, Uxbridge, UK*

(Accepted 27 September 2004)

Abstract
The purpose of this study was to capture the lower limb kinematics before during and after ball impact of soccer kicking by examining the influence of both sampling rate and smoothing procedures. Nine male soccer players performed maximal instep kicks and the three-dimensional leg movements were captured at 1000 Hz. Angular and linear velocities and accelerations were determined using four different processing approaches: processed using a modified version of a time-frequency filtering algorithm (WGN), smoothed by a second-order low-pass Butterworth filter at 200 Hz cut-off (BWF), re-sampled at 250 Hz without smoothing (RSR) and re-sampled at 250 Hz but filtered by the same Butterworth filter at 10 Hz cut-off (RSF). The WGN approach appeared to establish representative kinematics, whereas the other procedures failed to remove noisy oscillation from the baseline of signal (BWF), lost the peaks of rapid changes (RSR) or produced totally distorted movement patterns (RSF). The results indicate that the procedures used by some previous studies may have been insufficient to adequately capture the lower limb motion near ball impact. We propose a new time-frequency filtering technique as a better way to smooth data whose frequency content varies dramatically.

Keywords: *shank and foot kinematics, time frequency filtering, soccer kick, ball impact*

Introduction

Of the actions performed during soccer, kicking of the ball is the most important and studied skill. In particular, the movement characteristics of the kicking leg and their influence on ball speed have been investigated (Ansersen, Dörge, & Thomsen, 1999; Asami & Nolte, 1983; Barfield, 1995; Dörge, Andersen, Sørensen, & Simonsen, 2002; Isokawa & Lees, 1988; Lees, 1996; Lees & Nolan, 1998; Levanon & Dapena, 1998; Nunome, Asai, Ikegami, & Sakurai, 2002; Rodano & Tavana, 1993). Lower leg kinematics at or just before initial ball contact during kicking is important for determining both the quality of the impact and the resultant ball velocity (Asami & Nolte, 1983; Andersen *et al*., 1999; Dörge *et al*., 2002). Biomechanical data related to impacts involving large accelerations can be prone to error due to inadequate data processing (Knudson & Bahamonde, 2001) and sampling rates. The collection of kinematic data at high frame rates should minimize the error associated with the derivatives of displacement data (van den Bogert, 1994; Winter, 1990), but there is still the possibility of distortion if data containing movement transients are smoothed using traditional methods.

Studies that have documented kicking kinematics have typically captured limb movements at rates between 100 and 400 Hz (Andersen, *et al*., 1999; Barfield, 1995; Dörge *et al*., 2002; Isokawa & Lees, 1988; Lees, 1996; Lees & Nolan, 1998; Levanon & Dapena, 1998; Nunome *et al*., 2002; Rodano & Tavana, 1993; Teixeira, 1999) and then filtered the displacement data with a cut-off frequency of 6 – 18 Hz (Andersen *et al*., 1999; Dörge *et al*., 2002; Nunome *et al*., 2002; Teixeira, 1999). Although these methods were appropriate for describing the swing phase kinematics, it is unclear whether they can adequately capture and describe movement characteristics of the leg during ball contact. The duration of ball impact during instep kicking ranges between 9 and 12 $m \cdot s^{-1}$ and rapid deformations of the foot and ankle occur during this time (Asai, Akatsuka, & Kaga, 1995; Asami & Nolte, 1983). It is logical to assume

Correspondence: H. Nunome, Research Centre of Health, Physical Fitness and Sports, Nagoya University, Furo-cho, Chikusa, Nagoya 464-8601, Japan. E-mail: nunome@htc.nagoya-u.ac.jp

ISSN 0264-0414 print/ISSN 1466-447X online © 2006 Taylor & Francis
DOI: 10.1080/02640410400021450

that displacement data obtained in studies using lower sampling rates (100–200 Hz) (Barfield, 1995; Lees, 1996; Lees & Nolan, 1998; Rodano & Tavana, 1993; Teixeira, 1999) are unable to provide enough data points to adequately describe the curves for these short-duration, high-frequency movement characteristics. Furthermore, the filtering of low-frequency (swing phase) and high-frequency data (ball impact) together with a standard recursive Butterworth filtering approach is likely to distort kinematic information before and after impact (Knudson & Bahamonde, 2001). Digital low-pass filtering is commonly used in biomechanics (Winter, 1990). However, this type of filtering is inefficient when processing signals whose frequency content varies dramatically with time. It is also very difficult to achieve sufficient noise elimination while keeping the useful high frequencies intact, and therefore different cut-off frequencies must be applied at different times. Most previous studies of the ball kicking motion have failed to acknowledge this limitation (Andersen *et al.*, 1999; Barfield, 1995; Lees 1996; Lees & Nolan, 1998; Rodano & Tavana, 1993; Teixeira, 1999) and it is likely that leg swing motion immediately before ball impact has been inadequately documented.

Recently, new automatic time-frequency filtering approaches have become available to smooth displacement data that contain both low and high frequencies and so avoid such problems (Georgakis, Stergioulas, & Giakas, 2002a,b; Giakas, Stergioulas, & Vourdas, 2000). To date, no study has examined the influence of both sampling rate and data processing approaches on the kinematics of ball kicking or similar impacts. This study had three aims: (1) to illustrate more representative kinematics of the lower limb motion during ball kicking using high sampling rates and appropriate smoothing of the data; (2) to determine the effect of sampling and filtering frequency on the kinematic aspects of kicking; and (3) to re-examine the relationship between several kinematic variables associated with ball contact and resultant ball velocity.

Methods

Nine experienced male soccer players (age 27.6 ± 5.6 years, height 1.75 ± 0.06 m, mass 74.5 ± 8.2 kg) participated in the study after providing their informed written consent. Each participant preferred to kick the ball using his right leg. A FIFA-approved size five soccer ball (mass = 0.435 g) was used for each kicking session and its inflation was controlled throughout the trials at 650 hPa. To minimize the effect of type of shoe on the action of the lower leg, the same Astro Turf shoe (Umbro International; UK sizes 7–9; mass 405–431 g) was used.

After a brief warm-up, the participants performed at least nine consecutive, maximal-effort kicking trials. To maintain a straightforward ball trajectory, they were instructed to kick the ball as hard as possible into the centre of a goal (9 m in front of them) with the instep of their foot. A wooden target (1 m^2) was placed in the middle of the goal and kicks that either hit the target or came reasonably close to hitting the target were selected for analysis until nine successful shots were obtained.

Before the trials, reflective spherical markers (9 mm in diameter) were fixed securely (using acrylic glue) onto several bony anatomical landmarks, including the fifth metatarsal head, lateral side of the calcaneus, lateral malleolus, lateral head of the fibula, tibial tuberosity and the lateral side of the knee joint rotational centre (Figure 1a). The marker on the knee was expected to produce significant error due to skin movement relative to underlying bone compared with the other markers, which were located further from the joint (Lafortune, Lambert, & Lake, 1992). Thus, before the kicking trials, the position of the knee marker was recorded against three tracking markers on the shank (lateral malleolus, lateral head of the fibula and tibial tuberosity) in a static condition (standing position) and then it was removed.

Due to the minimal ball spin for this type of kicking, a flat, reflective marker (22 mm in diameter) was fixed to the centre of the ball to measure its displacement just after impact. The ball was sprayed with matt black paint beforehand to minimize extraneous reflections. Three-dimensional motions of the foot and shank before, during and after ball impact were recorded using a six-camera opto-electronic motion analysis system (ProReflex, Qualisys Inc., Sweden) operating at 1000 Hz. Displacement data were obtained continuously from 30 ms before ball impact to 30 ms after ball contact.

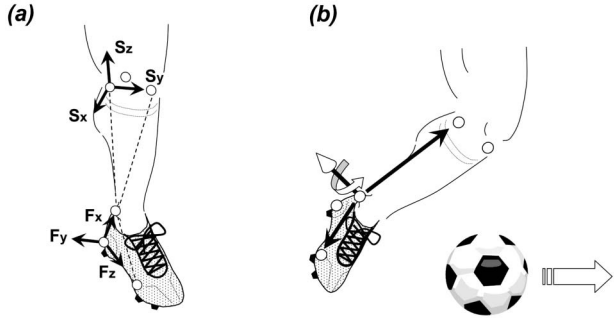

Figure 1. Definitions of local reference frames fixed to foot and shank (a) The magnitude of ankle angular velocity vector was calculated as a parallel component of the unit vector defined by the vector product of the vectors from the lateral malleolus to the lateral head of the fibula and from the lateral malleolus to the fifth metatarsal head (b).

Angular and linear kinematics

Three markers on each segment were used to define local reference frames fixed to the foot and shank segment as shown in Figure 1a. The position of the knee joint centre during kicking was estimated by the reference frame fixed to the shank. Absolute angular velocity vectors of the foot and shank segment were computed from these reference frames. For the differentiation, a single-step finite (forward) differentiation was used. The relative angular velocity vector of the foot segment was calculated by subtracting its absolute angular velocity vector from that of the shank segment. To measure anatomically relevant angular motion of the ankle with regard to dorsi-/plantar flexion, the magnitude of the relative foot angular velocity vector was calculated is a parallel component of the unit vector that was defined by the vector product of the vector from the lateral malleolus to the lateral head of the fibula and from the lateral malleolus to the fifth metatarsal head (Figure 1b). Positive and negative values correspond to dorsi- and plantar flexion, respectively. For shank angular velocity, its anatomically relevant axis could not be defined by the marker set used in the present study. Thus, shank angular velocity was represented by its absolute values, with positive and negative values corresponding to forward and backward shank swing, respectively. Angular accelerations of the ankle and shank were computed from the first derivatives of their angular velocities using a single-step finite (forward) differentiation. Linear velocities and accelerations of the toe (fifth metatarsal head), ankle (lateral malleolus) and knee (estimated from the local reference frame fixed to the shank) were derived from the first and second derivatives of their displacements, using a single-step finite (forward) differentiation.

Ball velocity and acceleration were calculated from non-filtered coordinates again using forward differentiation. The moment of impact was determined from the initial ball acceleration and defined as the frame before which there was a clear positive acceleration (above 200 $m \cdot s^{-2}$). The end of ball impact was defined as the last frame that demonstrated the positive acceleration above 200 $m \cdot s^{-2}$. Resultant peak ball velocity was computed as the average of five airborne frames after impact.

Automatic time-frequency filtering procedure

Georgakis *et al.* (2002a) described the design, operation and performance of a new time-frequency filtering algorithm based on the Wigner representation and then developed its automatic algorithm (Georgakis *et al.*, 2002b). They demonstrated considerably better estimates of peak velocity and acceleration in high-impact human motions. We have modified this algorithm and propose a new filtering scheme designed to address the problem of differentiating non-stationary signals that represent impacts of the human body with soft materials with no rebound. Details of the original algorithm are presented elsewhere (Georgakis *et al.*, 2002b). The modifications that enable the automatic selection of the filtering parameters of the present data are as follows:

1. The approximate timing of the centre of the impact event for filtering purposes can be estimated from the time when the second derivative reaches its peak. The signal is initially filtered (second-order dual-pass Butterworth filter, cut-off frequency 200 Hz) and then the second derivative can easily be calculated using finite differences, and its peak is clearly distinguishable. The cut-off frequency 200 Hz was chosen as it was the optimal frequency for both reducing the noise and keeping the acceleration peak distinguishable. Although this timing information is necessary for the application of the Wigner filtering algorithm, the selection of the cut-off frequency is not crucial in this estimation, provided that a reasonable value is chosen so that the acceleration peak is prominent and detectable. In the present study, the value 200 Hz was chosen after extensive experimentation with all the signals available. This value is ''optimal'' in the sense that it provided a clearly distinguishable acceleration peak for nearly all the signals.
2. The process of estimating the highest cut-off frequency during the ball impact phase exploits the relationship between the maximum acceleration (absolute values) present in the filtered signal and the cut-off frequency used. Initial investigation showed that, in most cases, the absolute peak acceleration of a low-pass-filtered version of the signal ascends rapidly (up to a certain point, where it gradually becomes approximately flat) as the low-pass cut-off increases. The ''optimum'' value of the filtering parameter occurs in this high cut-off ''plateau'' region. The algorithm performs iterative calculations of the absolute peak acceleration value around the estimated time of impact, using a third-order dual-pass Butterworth filter for incremental cut-off frequency values. The iteration stops when the rate of change falls below a pre-set level (in this case 60%) of the initial rate of change at a cut-off frequency of 10 Hz. The choice of the starting point for this iteration process (i.e. 10 Hz) is not crucial for the operation of the algorithm, provided that it is small enough (i.e. smaller than the actual cut-off

frequency to be determined at the point in time in question). The above approach for estimating the highest cut-off frequency was used to account for the presence of noise mainly at high frequencies.

The filtering algorithm operates on the raw displacement data of the toe (x, y and z component), heel (x, y and z component) and ankle (y and z component). The highest cut-off frequencies determined by the automatic algorithm were 72–247 Hz. The coordinates that did not possess clear peak accelerations during ball impact were filtered by a second-order dual-pass Butterworth filter operating at 83.3 Hz. As the y (antero-posterior) component of the toe marker is expected to have the highest frequency component, the cut-off frequency (83.3 Hz) was determined by using the residual analysis (Winter, 1990) between its first derivative and the cut-off frequencies.

To illustrate how the conventional Butterworth filtering approach and lower sampling rate typically used in previous studies influence the transient kinematic features of the distal segment around ball impact, the displacement data were processed using three approaches. First, the coordinates were smoothed by a second-order dual-pass Butterworth digital filter with a cut-off frequency of 200 Hz. This cut-off frequency was chosen because it was optimal for both reducing the noise and keeping the acceleration peak distinguishable (as used with the Wigner algorithm to allow the automatic selection of the timing of the impact). Second, the raw coordinates originally sampled at 1000 Hz were re-sampled at 250 Hz (every four frames) but not smoothed to assess the influence of the lower sampling rate typically reported in the literature (Barfield, 1995; Lees, 1996; Lees & Nolan, 1998; Rodano & Tavana, 1993; Teixeira, 1999). Third, the re-sampled data were then filtered with a second-order dual-pass Butterworth digital filter at 10 Hz to resemble typical sampling and filtering conditions used in previous studies (Lees, 1996; Lees & Nolan, 1998; Teixeira, 1999). To reduce the end-point problems, all signals filtered by the dual-pass Butterworth filter were extrapolated for 20 points by reflection before filtering and the extrapolated sequences were removed after filtering (Smith, 1989). Once the raw coordinate data for the lower leg and boot markers were filtered using the above approaches, angular and linear kinematic variables just before, during and after ball impact were computed. Foot velocity at ball impact was calculated as the velocity of the centre of gravity of the foot (defined as the mid-point between the toe and ankle makers) from which the velocity ratios between the foot and ball were computed in each data-processing condition.

Statistical analysis

The data were analysed statistically using analysis of variance followed by the Dunnett test for multiple comparisons between the variables. The first condition used the Wigner representation (WGN) filtering. The other three conditions were: (1) a conventional Butterworth filter at 200 Hz (BWF), (2) re-sampled (250 Hz) and non-filtered (RSR) and (3) re-sampled and filtered by a conventional Butterworth filter at 10 Hz (RSF). Statistical significance was set at $P < 0.05$ for all analyses.

Pearson correlation was also used to estimate the relationship between the kinematic variables and ball velocity using all trials (9×9) in each condition. The kinematic variables were treated as independent variables.

Results

The average resultant ball velocity was $26.3 \pm 3.4\ \mathrm{m \cdot s^{-1}}$ (range $19.2–32.6\ \mathrm{m \cdot s^{-1}}$) and the average contact time between the foot and ball during kicking was $9.1 \pm 0.7\ \mathrm{m \cdot s^{-1}}$. Large, high-frequency movements of the ankle and shank were detected during kicking in all participants. These movements were estimated to contain substantial frequency content up to 60 Hz. As shown in Figures 2a and 2b, the ankle was rapidly forced into plantar flexion by ball impact and reached its peak angular acceleration at the middle of ball contact and its peak plantar flexion velocity during the latter half of the ball contact phase. After this, the ankle was no longer angularly decelerated and began to flex dorsally just before the moment of ball release. In contrast, the shank was still angularly accelerating during the final phase of leg swing, and it is clear that peak positive (forward) angular velocity of the shank occurs at ball contact or in most cases after ball contact (see Figures 3a and 3b). After reaching peak negative angular velocity typically within a few milliseconds after ball contact, the shank was rapidly angularly decelerated and reached its peak negative angular acceleration just before ball release. The shank continued to decelerate after ball release for about 4–5 ms before reaching its minimum positive angular velocity.

The toe experienced a large linear deceleration after ball impact, followed by an increased deceleration of the ankle, with little disturbance of the motion at the level of the knee (see Figures 4a and 4b).

After WGN and BWF processing, the angular and linear velocity and acceleration curves matched closely the changes during ball contact seen in the raw, unsmoothed 1000 Hz data (see Figures 2–4). As expected, the RSR data did not show the sudden changes in ankle angular velocity and toe linear

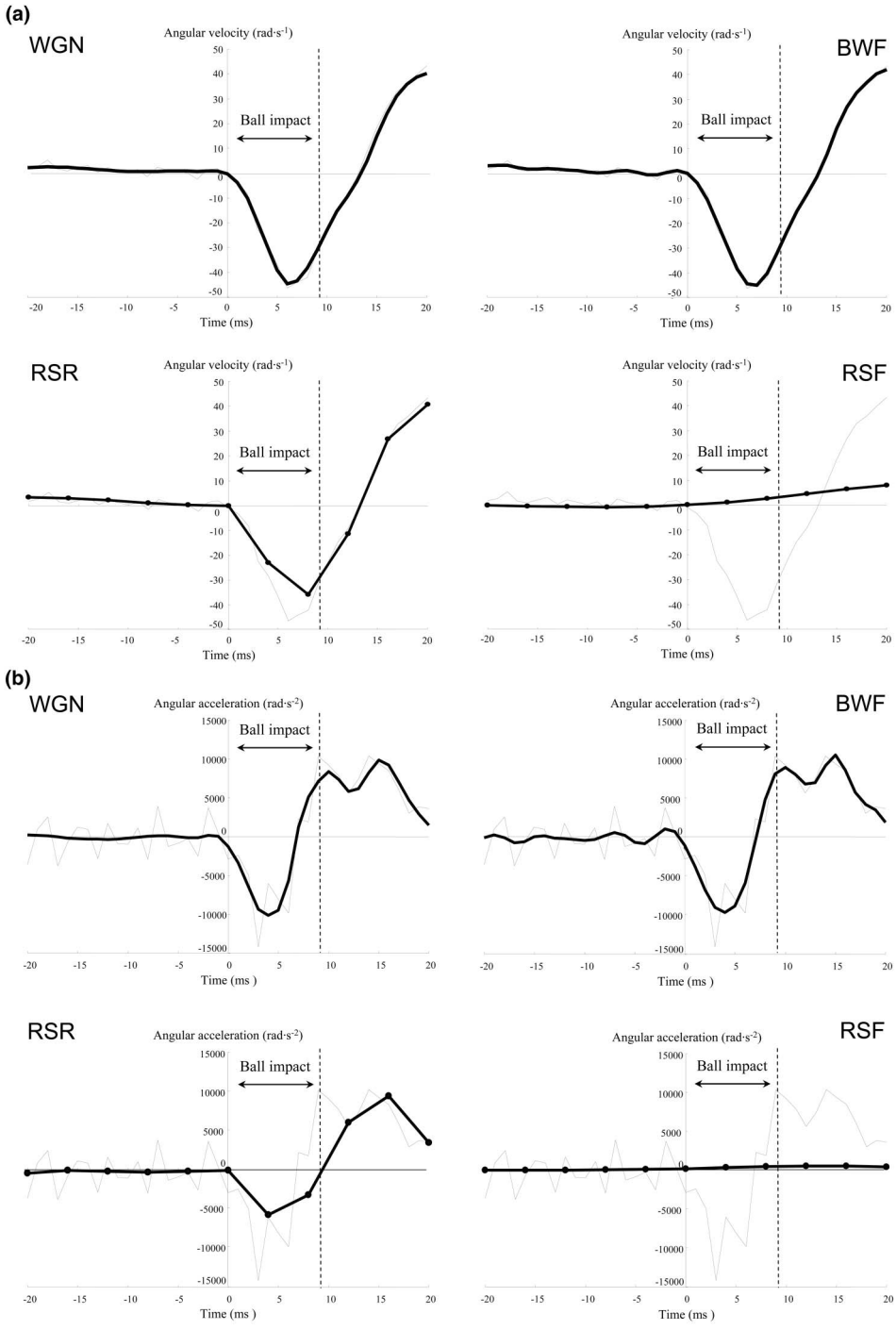

Figure 2. Comparison of changes in angular velocity (a) and angular acceleration (b) of the ankle at ball impact computed from four different filtering and sampling techniques (WGN, BWF, RSR and RSF). Typical changes (thick solid line) are shown against the original raw change (thin solid line).

velocity after ball impact and these trends were more obvious for the second derivatives (angular and linear accelerations). The peak ankle plantar flexion angular velocity was significantly underestimated and the knee linear velocity at ball impact was significantly overestimated compared with the WGN data (see Table I). Most second derivative values were significantly different from those of the WGN data, except for the values at ball impact of ankle angular acceleration, shank angular acceleration and knee linear acceleration (see Table II). Furthermore, the RSF data demonstrated totally different patterns, in which the high-frequency movement transients were removed completely, and also distorted the values at initial ball impact (see Figure 2–4). This effect was most marked for the ankle joint motion where the

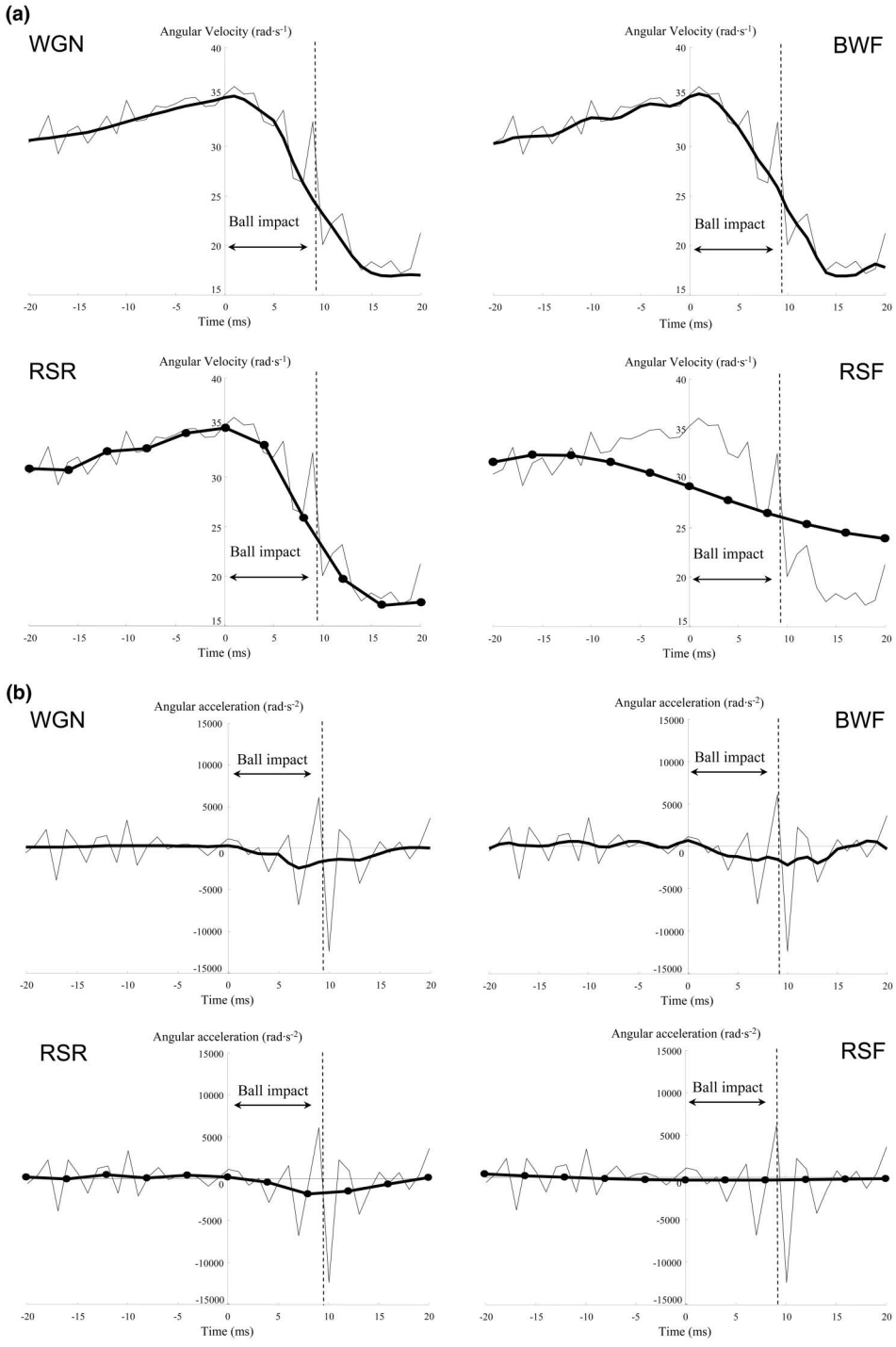

Figure 3. Comparison of changes in angular velocity (a) and angular acceleration (b) of the shank at ball impact computed from four different filtering and sampling techniques (WGN, BWF, RSR and RSF). Typical changes (thick solid line) are shown against the original raw change (thin solid line).

rapid plantar flexion motion observed in the raw data was absent using the RSF method of data processing (see Figure 2a and 2b). The first derivative values were significantly underestimated compared with those obtained with the WGN approach apart from knee linear velocity, which was significantly overestimated (see Table I). Significant differences were also found for all second derivative values between the RSF and WGN methods (see Table II). This is especially evident when viewing the toe velocity and acceleration curves (see Figures 4a and 4b) where toe velocity is falsely shown to decelerate as the foot approaches the ball, when in fact the toe continued to accelerate until ball impact (WGN and BWF). In

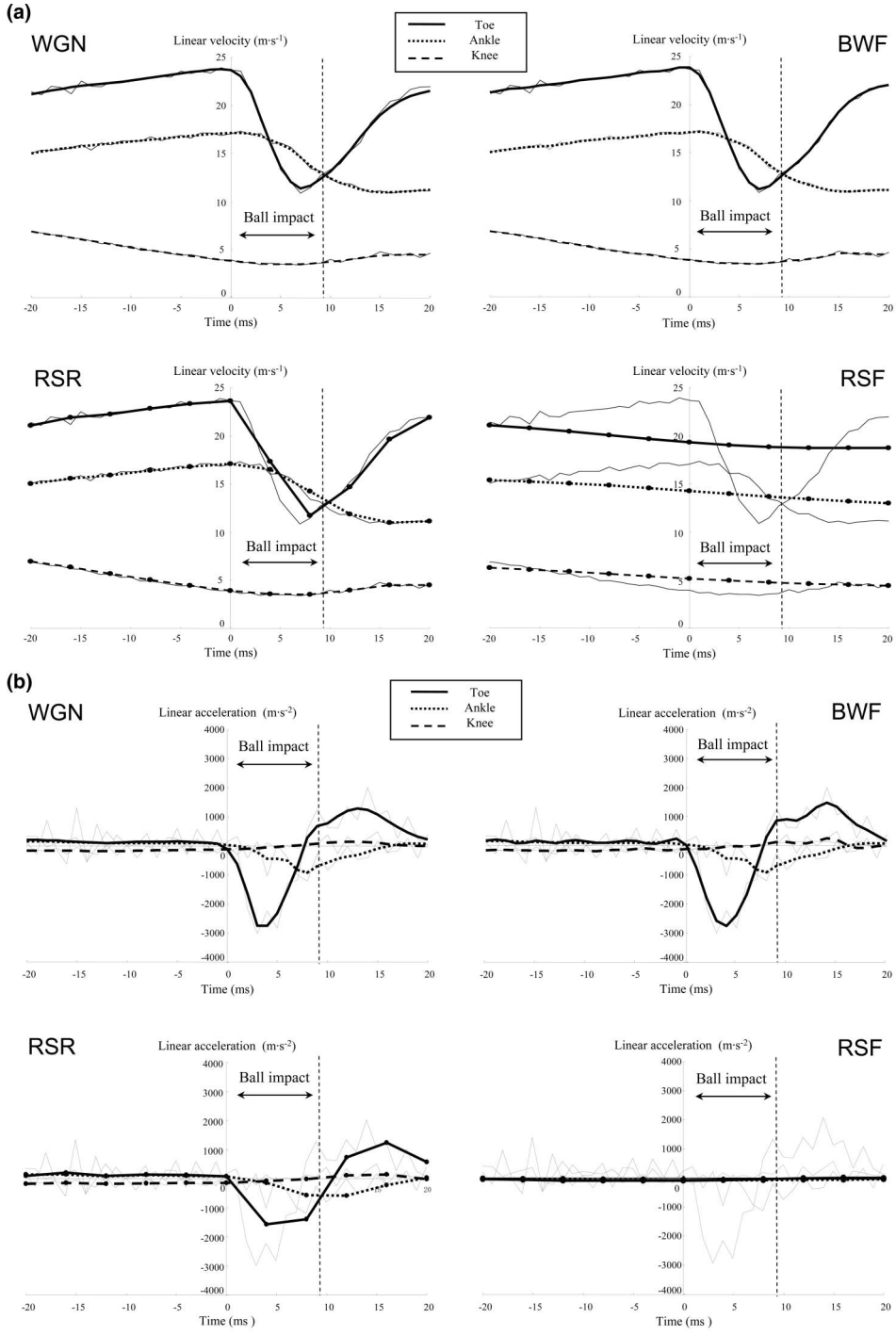

Figure 4. Comparison of changes in linear velocity (a) and linear acceleration (b) of the toe, ankle and knee at ball impact computed from four different filtering and sampling techniques (WGN, BWF, RSR and RSF). Typical changes of the toe (thick solid line), ankle (dotted line) and knee (dashed line) are shown against the original raw change (thin solid line).

contrast, the value of knee velocity at ball impact was significantly overestimated using the RSF method. The foot-to-ball velocity ratio using the RSF approach also showed a significantly larger value compared with the WGN approach (see Table I).

Although the movement transients using BWF processing appeared to follow the raw changes through the ball impact phase (similar to the WGN approach), they still possessed appreciable noise in the low-frequency movement phase (baseline) before ball impact. This oscillation was more evident in the second derivative values (Figures 2b, 3b and 4b). Significant differences were found between the WGN and BWF approaches for peak shank angular

Table I. Summary of selected velocity parameters in each data-processing condition (mean ± *s*)

	WGN	BWF	RSR	RSF
Ankle angular velocity at ball impact ($rad \cdot s^{-1}$)	−0.8 ± 3.9	−0.5 ± 4.2	−1.7 ± 7.5	−2.3 ± 3.8*
Shank angular velocity at ball impact ($rad \cdot s^{-1}$)	35.8 ± 4.6	36.2 ± 4.7	35.5 ± 4.7	29.0 ± 4.0*
Max. ankle angular velocity ($rad \cdot s^{-1}$)	−42.4 ± 12.7	−44.1 ± 12.8	−35.5 ± 12.1*	−2.4 ± 3.8*
Max. shank angular velocity ($rad \cdot s^{-1}$)	36.0 ± 4.6	37.0 ± 4.8*	36.4 ± 4.6	32.6 ± 4.6*
Toe velocity at ball impact ($m \cdot s^{-1}$)	22.0 ± 2.2	22.1 ± 2.3	21.7 ± 2.5	17.6 ± 1.7*
Ankle velocity at ball impact ($m \cdot s^{-1}$)	16.9 ± 1.8	16.9 ± 1.8	16.7 ± 1.8	13.9 ± 1.4*
Knee velocity at ball impact ($m \cdot s^{-1}$)	4.8 ± 0.9	4.8 ± 0.9	5.0 ± 0.9*	5.6 ± 0.8*
Ball–foot velocity ratio	1.35 ± 0.09	1.34 ± 0.09	1.36 ± 0.10	1.66 ± 0.13*

* Significant difference by Dunnet test for multiple comparisons between WGN and the other techniques ($P < 0.05$). WGN = time-frequency filtering algorithm; BWF = smoothing with a second-order low-pass Butterworth filter at a cut-off frequency of 200 Hz; RSR = re-sampling at 250 Hz without smoothing; RSF = re-sampling at 250 Hz and smoothed with a second-order Butterworth filter at a cut-off frequency of 10 Hz.

Table II. Summary of selected acceleration parameters in each data-processing condition (mean ± *s*)

	WGN	BWF	RSR	RSF
Ankle angular acceleration at ball impact ($rad \cdot s^{-1}$)	−375.9 ± 741.6	43.2 ± 813.8*	−232.5 ± 872.4	87.7 ± 136.8*
Shank angular acceleration at ball impact ($rad \cdot s^{-1}$)	137.0 ± 187.1	178.9 ± 759.5	197.5 ± 345.3	−333.1 ± 169.1*
Max. ankle angular acceleration ($rad \cdot s^{-1}$)	−11820.1 ± 2599.2	−11253.8 ± 2130.2	−6335.2 ± 2052.0*	−156.8 ± 234.8*
Max. shank angular acceleration ($rad \cdot s^{-1}$)	−2608.5 ± 731.6	−2813.3 ± 993.0*	−1966.3 ± 535.8	−366.4 ± 194.7*
Toe acceleration at ball impact ($m \cdot s^{-1}$)	−40.6 ± 148.9	−11.6 ± 202.7	78.5 ± 162.6*	110.3 ± 37.1*
Ankle acceleration at ball impact ($m \cdot s^{-1}$)	50.7 ± 43.9	72.2 ± 64.3	94.0 ± 42.9*	−72.2 ± 33.7*
Knee acceleration at ball impact ($m \cdot s^{-1}$)	−1120.0 ± 52.1	−119.2 ± 67.6	−117.0 ± 49.2	−64.3 ± 26.2*
Max. toe acceleration ($m \cdot s^{-2}$)	−2535.1 ± 576.4	−2438.3 ± 515.8	−1681.4 ± 290.7*	−115.0 ± 40.6*
Max. shank acceleration ($m \cdot s^{-2}$)	−1020.0 ± 282.2	−967.4 ± 197.8	−711.0 ± 129.0*	−87.2 ± 35.3*

* Significant difference by Dunnet test for multiple comparisons between WGN and the other techniques ($P < 0.05$). WGN = time-frequency filtering algorithm; BWF = smoothing with a second-order low-pass Butterworth filter at a cut-off frequency of 200 Hz; RSR = re-sampling at 250 Hz without smoothing; RSF = re-sampling at 250 Hz and smoothed with a second-order Butterworth filter at a cut-off frequency of 10 Hz.

velocity, peak shank angular acceleration and ankle angular acceleration at ball impact (see Tables I and II). The appreciable oscillation is most likely responsible for these significant differences.

Consistent trends were observed in all conditions except for the relationship between knee linear velocity and the resultant ball velocity. The toe and ankle linear velocities at ball impact were strongly correlated (r = 0.712 to 0.848; r^2 = 0.507 to 0.719) with final ball speed in all conditions (see Table III). However, the RSF condition showed a strong correlation (r = 0.705; r^2 = 0.497) between knee linear velocity and ball speed. In contrast, for the relationship between angular velocity (peaks and the values at ball impact) and ball speed, the WGN and BWF approaches consistently showed significant but relatively weak correlations (r = − 0.225 to 0.606; r^2 = 0.050 to 0.367), and the RSR and RSF approaches showed several non-significant correlations (r = − 0.027 to − 0.115; r^2 = 0.001 to 0.013) (see Table III).

Discussion

Effect of sampling rate and filtering procedure

Using a new automatic version of the time-frequency filtering technique (Georgakis *et al*., 2002b) and high sampling rates of displacement data (1000 Hz), this study has clearly demonstrated the presence of rapid, high-frequency movement characteristics of the foot, ankle and shank during ball kicking that were not made apparent using traditional data collection (displacement sampling 250 Hz) and processing (dual-pass Butterworth digital filtering with constant cut-off frequency at 10 Hz) procedures. The present study succeeded in establishing more representative kinematics of the lower leg motion during both the sudden transition phase from leg swing to ball impact phase.

The sudden decceleration caused by ball impact is a difficult phase to capture adequately, which may cause a systematic error in its derivative parameters in the last few frames before ball impact. Moreover,

the area of distortion would be expanded if conventional filtering were applied to the data. Some authors (Levanon & Dapena, 1998; Nunome *et al.*, 2002) have tried to address this problem using extrapolation or filtering in the forward direction only. However, in the case of Levanon and Dapena (1998), it still left open the possibility of larger random errors near ball impact. Also, the forward pass filtering technique (Nunome *et al.*, 2002) could not eliminate the effect of the phase distortion on the data. Most ball kicking studies have failed to acknowledge this type of potential error (Andersen *et al.*, 1999; Barfield, 1995; Isokawa & Lees, 1988; Lees, 1996; Lees & Nolan, 1998; Rodano & Tavana, 1993; Teixeira, 1999), and it is often unclear how displacement coordinates were smoothed (Isokawa & Lees, 1988; Lees, 1996; Lees & Nolan, 1998; Rodano & Tavana, 1993). In this study, we found that when a conventional Butterworth filter with a typical 10 Hz cut-off frequency was applied to the re-sampled data (the RSF approach), angular and linear transient changes were seriously distorted and completely different curves were created. The over-smoothing observed with the RSF approach removed totally the rapid foot plantar flexion motion during ball contact and falsely showed an apparent deceleration (angular and linear) of the shank before the moment of ball impact. Knudson and Bahamonde (2001) showed, using a tennis impact, that if the angular and linear data are smoothed through impact using conventional Butterworth filtering, a false peak before ball impact is introduced by over-smoothing. It is reasonable to assume that a similar type of distortion would be produced with the instep kick. With the RSF approach, distortion caused most kinematic variables to be significantly underestimated (except knee linear velocity, which was overestimated) compared with the WGN approach. Although an insufficient sampling rate (250 Hz) and over-smoothing (10 Hz) may account for this, the distortion caused by the over-smoothing seemed to be more crucial. These results indicate that the procedures, sampling rates and filtering techniques used by some previous studies (e.g. Barfield, 1995; Lees, 1996; Teixeira, 1999) may have been insufficient to adequately capture motion of the shank and foot during kicking, especially near of ball impact.

Using a Butterworth filter with a high cut-off frequency (facilitated by using a high sampling rate) allowed transient joint motions during ball impact to be tracked sufficiently, although appreciable oscillations were detected on the baseline of the signals (see Figures 2–4). Significant differences were observed for both the first (the peak shank angular velocity) and second derivatives (the peak shank angular acceleration and ankle angular acceleration at ball impact) compared with the WGN approach (see Tables I and II). If these oscillations are derived from noise, they can be erased when signals are simply averaged. To examine this issue, the shank angular velocity changes over nine trials of a typical participant were simply averaged and then compared with a typical single trial using two different approaches (WGN and BWF). As shown in Figure 5, the oscillations observed at baseline in the BWF case were almost completely removed when nine signals were simply averaged and the averaged curve was very similar to that of the WGN case. In contrast, for the WGN case, these small oscillations were not detected in either single trials or the averaged signal. Thus, it can be assumed that the oscillations observed for the BWF case are due to noise for the most part, and the conventional filtering procedure with a high cut-off frequency (200 Hz) failed to remove it. The time-frequency filtering procedure conducted in the present study (WGN) succeeded in removing noise in the pre-impact swing phase, yet maintained the peak of the rapid change during the ball impact phase, thereby demonstrating a distinct advantage in accurately characterizing the motion characteristics involved in this action. It is important to emphasize that the time-frequency filtering algorithm used in the present study is automated and the cut-off frequency is optimized for each signal, whereas the constant 200 Hz cut-off frequency in the BWF approach may not have been optimal for all signals. The automatic algorithm worked well without any modifications for all kicks of all participants, by filtering different markers/positions on the body.

The ratio between the final foot velocity at ball contact and the resultant ball velocity has been widely calculated. Generally, the values are greater than unity and have ranged from 1.06 (Asami & Nolte, 1983) to 1.29 (Plagenhof, 1971). Isokawa and Lees (1988) showed that the variation in the ratio is dependent on what part of the foot is used to calculate foot velocity. They reported that the ratio can be as high as 1.65 when the ankle is used to calculate foot velocity. Previous studies that used reliable filtering techniques (Levanon & Dapena, 1998, Nunome *et al.*, 2002) reported intermediate values ($\sim$ 1.38). Similar values were obtained in this study apart from the RSF approach (see Table I), which showed a distinctly higher value (1.66) that was even higher than the ankle-to-ball velocity ratio (Isokawa & Lees; 1988).

The correlation coefficients between ball and foot speed have been shown to vary from 0.49 (Rodano & Tavana, 1993) to 0.83 (Levanon & Dapena, 1998). The results of the present study confirm that both toe and ankle linear velocity at ball impact are highly correlated with ball velocity and the strong relationships were consistent over the four different sampling

Table III. Summary of correlation coefficients between resultant ball velocity and selected velocity parameters in each data-processing condition.

	WGN		BWF		RSR		RSF	
	r	r^2	*r*	r^2	*r*	r^2	*r*	r^2
Ankle angular velocity at ball impact	−0.225	0.050	−0.363	0.132	-0.115^{ns}	0.013^{ns}	-0.027^{ns}	0.001^{ns}
Shank angular velocity at ball impact	0.606	0.367	0.574	0.329	0.592	0.351	0.552	0.305
Max. ankle angular velocity	0.435	0.189	0.484	0.234	0.544	0.296	-0.023^{ns}	0.001^{ns}
Max. shank angular velocity	0.584	0.341	0.484	0.234	0.525	0.276	0.552	0.305
Toe velocity at ball impact	0.802	0.643	0.805	0.647	0.712	0.507	0.751	0.564
Ankle velocity at ball impact	0.846	0.716	0.848	0.719	0.835	0.697	0.799	0.638
Knee velocity at ball impact	0.443	0.196	0.437	0.191	0.505	0.255	0.705	0.497

[ns] Non-significant correlation with resultant ball velocity. WGN = time-frequency filtering algorithm; BWF = smoothing with a second-order low-pass Butterworth filter at a cut-off frequency of 200 Hz; RSR = re-sampling at 250 Hz without smoothing; RSF = re-sampling at 250 Hz and smoothed with a second-order Butterworth filter at a cut-off frequency of 10 Hz.

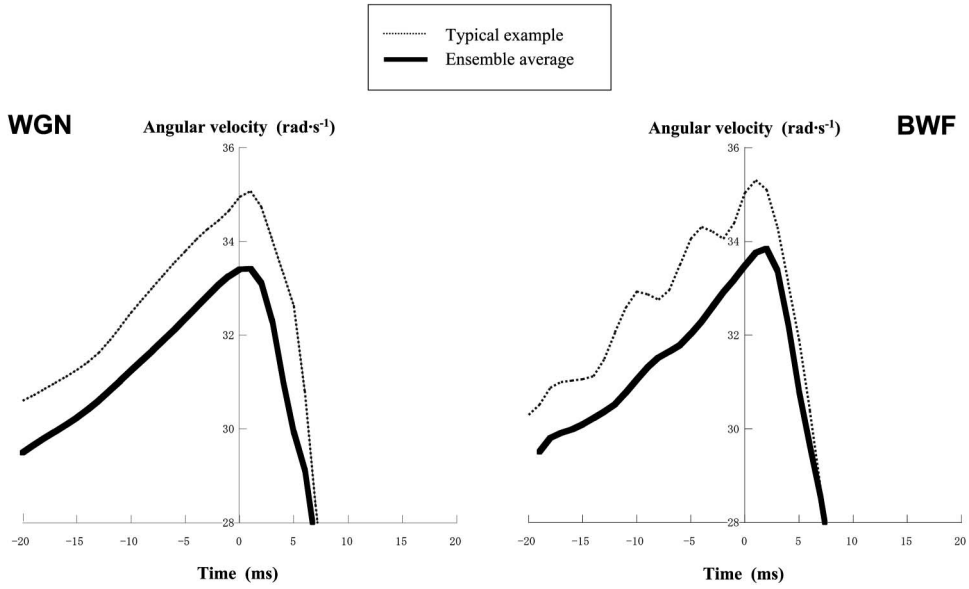

Figure 5. Comparison of averaged (± *s*), and one representative example of, changes in shank angular velocity between two different filtering techniques (WGN and BWF). The enlarged average and typical curves are shown by thick solid and dotted lines, respectively.

and filtering conditions (see Table II). Linear velocity of the foot was seriously distorted around impact with the RSF approach and although it still correlated with measures of ball velocity, the correlations could not predict the magnitude of ball velocity. The moderate correlation ($r = 0.61$) between the ball and maximum knee linear velocities reported by Barfield (1995) is not supported by our findings and was probably due to insufficient sampling speed (200 Hz) and filtering techniques.

Representative kinematics

The angular and linear motions of the distal segment in kicking have been illustrated by several authors, who observed apparent linear and angular decelerations before ball impact (Barfield, 1995; Dörge *et al.*, 2002; Lees, 1996, Lees & Nolan, 1998; Teixeira, 1999). The nature of the leg swing observed in the final phase of kicking has led to a proposed accuracy-enhancing strategy of motor control (Teixeira, 1999). However, changes in angular and linear velocity and acceleration observed in the present study (see Figures 2–4) were very different than those reported previously, and in contrast to the proposed strategy of kicking. The shank was still angularly accelerating and the ankle was still linearly accelerating until the moment of ball impact, both of which reached their peak angular and linear velocity after ball impact, respectively after ball impact. As described above, adequate sampling speeds and

filtering techniques succeeded in illustrating the swing motion of the distal segment more accurately.

On the field, coaches often advise players to 'kick through the ball', although there is no evidence to support this type of instruction from a biomechanical perspective. The present study is the first to provide evidence that strongly supports the above practical advice of kicking by revealing the 'more representative' distal segment motion before, during and after ball contact.

The nature of ankle and shank motions suggests several unknown aspects of ball impact dynamics during the soccer instep kick. The shank was still angularly decelerating after the foot was no longer in contact with the ball. During this phase, the shank angular motion was mainly influenced by a combination of two factors: the moment acting on its proximal end and inertial motion of the shank itself. Although the nature and magnitude of the moment (assumed to act to accelerate the shank) are unknown, it may be assumed that the effect of the inertial motion of the shank was still apparent immediately after ball contact.

The rapid deformations of the foot and ankle on ball impact are influenced by several factors, including soccer shoe sole stiffness and rigidity of the ankle joint (Asai *et al.*, 1995). Asai and colleagues demonstrated that the foot segment can be considered to be fairly rigid up to the fifth metatarsal head and consequently reflects well the motion of the ankle. The deformation rates are probably dependent on the interaction between shoe and ankle stiffness characteristics with neuromuscular factors perhaps even playing a role (Hennig, 1998). Authors who have tried to quantify ankle deformation during ball impact have indicated that the rapid plantar flexion of the ankle joint is probably 'forced' even in a skilled population (Asai *et al.*, 1995; Asami & Nolte, 1983; Ben-Sira, 1980). The present study confirmed the rapid plantar flexion of the ankle joint to the extreme range of motion seen among mature soccer players. As this motion occurs within a few milliseconds of the moment of ball contact while the shank is still angularly accelerating, it is reasonable to assume that the rapid ankle plantar flexion motion is totally passive, thus mainly absorbing the initial impact force and being dependent upon the initial conditions of impact and characteristics of the impacting interface.

Forced, rapid ankle plantar flexion after ball impact was consistently observed for all participants and the commonly held notion among coaches that the ankle joint should be firmly fixed to provide a better ball impact for delivering faster ball speeds appears to need revision. For example, the participant who produced a relatively high ball velocity ($32.6\ m \cdot s^{-1}$) also demonstrated substantial ankle plantar flexion on ball impact. The procedures used in the present study will allow closer examination of the foot–ball interaction during this sudden transient loading phase (from swing to ball impact).

The repetitive forced ankle motion into extreme plantar flexion during kicking has been linked to the development of footballer's ankle (Massada, 1991; McMurray, 1950; O'Neill, 1981). This is a condition where bone is remodelled at the front and rear of the ankle joint causing reduced mobility and sometimes chronic pain. Some abnormality in osseous development around the ankle joint is very common even in young players and may represent a natural adaptation to the frequent, high transient stresses imposed during kicking (Biedert, 1993, Massada, 1991). Eventually, mobility may be compromised enough to have a negative effect on agility and performance. To date, only one study has tried to explain the relationship between foot deformation and this ankle impingement syndrome using kinematic variables (Johannes, Slim, Van Soest, & Van Dijk, 2002). This type of study can provide more relevant information related to the exact cause of footballer's ankle. The accurate quantification of the rapid ankle movements during kicking is an important first step in determining the relative importance of factors such as soccer boot stiffness and initial ankle joint stiffness on repetitive trauma to the joint. To help quantify the transient stresses on bone and ligaments, it is crucial to have an accurate representation of lower limb kinematics during the sudden transition from unloaded to high loaded conditions. Such movement transients can be determined effectively and automatically using the procedures documented in this paper.

Conclusions

Representative impact phase kinematics of the instep soccer kick were revealed in the present study using high sampling rates of displacement data (1000 Hz) and a new filtering procedure (time-frequency filtering). The time-frequency filtering procedure demonstrated a distinct advantage in removing noise during the pre-impact swing phase, yet maintained the peak values of high-frequency movement transients during the ball impact phase. Although the use of high-speed sampling and conventional filtering with a high cut-off frequency failed to remove low-frequency noise during the swing phase, it offered an alternative approach to capture the high-frequency movement transients during ball impact.

Acknowledgement

The authors thank Rumi Kozakai for her suggestions and assistance with the statistical analysis.

References

Andersen, T. B., Dörge, H. C., & Thomsen, F. I. (1999). Collisions in soccer kicking. *Sports Engineering*, *2*, 121–125.

Asai, T., Akatsuka, T., & Kaga, M. (1995). Impact process of kicking in football. In K. Hakkinen, K. L. Keskinen, P. V. Komi, & A. Mero (Eds.), *Proceedings of the XVth Congress of the International Society of Biomechanics* (pp. 74–75). Jyvaskyla: Gummerus Printing.

Asami, T., & Nolte, V. (1983). Analysis of powerful ball kicking. In H. Matsui & K. Kobayashi (Eds.), *Biomechanics VIII-B* (pp. 695–700). Champaign, IL: Human Kinetics.

Barfield, W. R. (1995). Effects of selected kinamatic and kinetic variables on instep kicking with dominant and nondominant limbs. *Journal of Human Movement Studies*, *29*, 251–272.

Ben-Sira, D. (1980). *A comparison of the mechanical characteristics of the instep kick between skilled soccer players and novices*. Unpublished doctoral dissertation. University of Minnesota.

Biedert, R. (1993). Anterior ankle pain in football: Aetiology and indications for arthroscopic treatment. In T. Reilly, J. Clarys, & A. Stibbe (Eds.), *Science and football II* (pp. 396–401). London: E & FN Spon.

Dörge, H. C., Andersen, T. B., Sørensen, H., & Simonsen, E. B. (2002). Biomechanical differences in soccer kicking with the preferred and the non-preferred leg. *Journal of Sports Sciences*, *20*, 293–299.

Georgakis, A., Stergioulas, L. K., & Giakas, G. (2002a). Winger filtering with smooth roll-off boundary for differentiation of noisey non-stationary signals. *Signal Processing*, *82*, 1411–1415.

Georgakis, A., Stergioulas, L. K., & Giakas, G. (2002b). An automatic algorithm for filtering kinematic signals with impact in the Winger representation. *Medical and Biological Engineering and Computing*, *40*, 625–633.

Giakas, G., Stergioulas, L. K., & Vourdas, A. (2000). Time-frequency analysis and filtering of kinematic signals with impacts using the Wigner function: Accurate estimation of the second derivative. *Journal of Biomechanics*, *33*, 567–574.

Hennig, E. (1998). Measuring methods for the evaluation of soccer shoe properties. In *Proceedings of the Soccer Science and Technology Congress* (pp. 299–310). Lyons: Centre Technique Cuir Chausure Maroquinerie.

Isokawa, M., & Lees, A. (1988). A biomechanical analysis of the instep kick motion in soccer. In T. Reilly, A. Lees, K. Davids, & W. J. Murphy (Eds.), *Science and football* (pp. 449–455). London: E & FN Spon.

Johannes, L. T., Slim, E., Van Soest, A. J., & Van Dijk, C. N. (2002). The relationship of the kicking action in soccer and anterior ankle impingement syndrome: A biomechanical analysis. *American Journal of Sports Medicine*, *30*, 45–50.

Knudson, D., & Bahamonde, R. (2001). Effect of endpoint conditions on position and velocity near impact in tennis. *Journal of Sports Sciences*, *19*, 839–844.

Lafortune, M. A., Lambert, C., & Lake, M. (1992). Skin marker displacement at the knee joint. In *Proceedings of NACOB II, the Second North American Congress on Biomechanics* (pp. 101–102). Chicago, IL: NACOB Organizing Committee.

Lees, A. (1996). Biomechanics applied to soccer skills. In T. Reilly (Ed.), *Science and football (soccer)* (pp. 123–134). London: E & FN Spon.

Lees, A., & Nolan, L. (1998). The biomechanics of soccer: A review. *Journal of Sports Sciences*, *16*, 211–234.

Levanon, J., & Dapena, J. (1998). Comparison of the kinematics of the full-instep and pass kicks in soccer. *Medicine and Science in Sports Exercise*, *30*, 917–927.

Massada, J. L. (1991). Ankle overuse injuries in soccer players: Morphological adaptation of the talus in the anterior impingement. *Journal of Sports Medicine and Physical Fitness*, *31*, 447–451.

McMurray, T. P. (1950). Footballer's ankle. *Journal of Bone and Joint Surgery*, *32B*, 68–69.

Nunome, H., Asai, T., Ikegami, Y., & Sakurai, S. (2002). Three-dimensional kinetic analysis of side-foot and instep soccer kicks. *Medicine and Science in Sports Exercise*, *34*, 2028–2036.

O'Neill, T. (1981). Soccer injuries. In T. Reilly (Ed.), *Sports fitness and sports injuries* (pp. 127–132). London: Faber & Faber.

Plagenhof, S. (1971). *Patterns of human motion* (pp. 98–117). Englewood Cliffs, NJ: Prentice-Hall.

Rodano, R., & Tavana, R. (1993). Three dimensional analysis of the instep kick in professional soccer players. In T. Reilly, J. Clarys, & A. Stibbe (Eds.), *Science and football II* (pp. 357–361). London: E & FN Spon.

Smith, G. (1989). Padding point extrapolation techniques for the Butterworth digital filter. *Journal of Biomechanics*, *22*, 967–971.

Teixeira, L. A. (1999). Kinematics of kicking as a function of different sources of constraint on accuracy. *Perceptual and Motor Skills*, *88*, 785–789.

Van den Bogert, A. J. (1994). Analysis and simulation of mechanical loads on human musculoskeletal system: A methodological overview. *Exercise and Sport Sciences Reviews*, *22*, 23–51.

Winter, D. A. (1990). *Biomechanics and motor control of human movement*. New York: Wiley.